HHS Public Access

Author manuscript

ChemMedChem. Author manuscript; available in PMC 2017 August 19.

Published in final edited form as:

ChemMedChem. 2016 August 19; 11(16): 1752–1761. doi:10.1002/cmdc.201600140.

Cyclic-ketoximes as ER beta-selective agonists

Dr. Carlotta Granchi[a], **Margherita Lapillo**[a], **Concetta Russo Spena**[b], **Dr. Flavio Rizzolio**[c], **Prof. Dr. Tiziano Tuccinardi**[a], **Dr. Teresa A. Martin**[d], **Kathryn E. Carlson**[d], **Prof. Dr. John A. Katzenellenbogen**[d], and **Prof. Dr. Filippo Minutolo**[a]

Carlotta Granchi: carlotta.granchi@farm.unipi.it

[a]Dipartimento di Farmacia, Università di Pisa, Via Bonanno 33, 56126 Pisa, Italy

[b]Graduate School in Chemistry, University of Trieste, Italy

[c]Division of Experimental and Clinical Pharmacology, Department of Molecular Biology and Translational Research, CRO National Cancer Institute and Center for Molecular Biomedicine, IRCCS 33081 Aviano, Pordenone, Italy

[d]Department of Chemistry, University of Illinois, 600 S. Mathews Avenue, Urbana, IL 61801, USA

Abstract

The development of selective ERβ-agonists represents a therapeutic strategy against several kinds of cancers, but the high homology between the two receptor subtypes, ERα and ERβ, makes the achievement of this goal very challenging. In the past, we developed salicylaldoxime- and salicylketoxime-based molecules which proved to bind well to ERβ. In this paper, a further structural evolution of salicylketoximes is presented: two of the newly synthesized five-membered cyclic ketoximes bind with nanomolar affinities to ERβ, and they show selectivity for this subtype over ERα. Their agonist character was confirmed by cell-free coactivator recruitment assays in which we demonstrated the ability of these compounds to form an active complex with ERβ capable of recruiting coactivator proteins, indicating their efficacy as agonists. Finally, their potency and selectivity for ERβ binding were rationalized by molecular modeling studies.

What a nice cycle tour!

Correspondence to: Carlotta Granchi, carlotta.granchi@farm.unipi.it.

Supporting information for this article is given via a link at the end of the document.

A new class of ERβ agonists was developed by introducing a cyclic portion in the salicylketoxime scaffold. This structural modification gave rise to potent and selective ligands for ERβ. Cell-free coactivator binding and recruitment assays proved that ERβ was able to recruit coregulator proteins upon ligand activation, confirming the agonist functional properties of these compounds.

Keywords

cancer; receptors; oxime; estrogen; binding

Introduction

Estrogen receptors (ERs) are nuclear transcription factors responsible for the regulation of many physiological processes, such as cell growth, reproduction, development and differentiation.[1] In response to the steroidal hormones, estrogens, these receptors bind with high affinity to specific DNA sequences called estrogen response elements (EREs) and modulate gene expression. Two receptor subtypes are known, ERα and ERβ, and they have different tissue distribution patterns in the human body. ERα is mainly expressed in reproductive tissues (uterus, ovary) and in breast, whereas ERβ is the principal subtype in certain regions of the central nervous system, in lung, prostate, colon, kidney and the immune system. In particular, ERα expression generally increases at early stages of certain cancers, and acts as a tumor promoter, while the low levels of ERβ during carcinogenesis and cancer progression confirm that this receptor may act as a tumor suppressor. In fact, the antiproliferative effect exerted by ERβ was observed in several types of cancers, such as, for example, breast,[2] prostate,[3] colon,[4] renal,[5] pleural mesothelioma,[6] and glioma.[7] Therefore, since the discovery of ERβ in 1996,[8] a great interest has been focused on the search for molecules that are able to selectively interact with this receptor,[9] since ERβ-selective agonists have therapeutic potential for use in cancer therapy. ERβ-selective activation is expected to produce beneficial effects that would be free from the undesired ERα-mediated proliferative effects on breast and uterus. Unfortunately, the development of ERβ-selective ligands has proved to be very challenging due to the high similarity of the two

receptor subtypes. ERα and ERβ share only a limited amino acid sequence identity (59%) in their ligand binding domains (LBDs), but the differences within their respective ligand binding cavities are limited to only two amino acid positions; in particular Leu384 and Met421 in ERα are replaced by Met336 and Ile373, respectively, in ERβ. These slight differences together with minor alterations of tertiary structure of the LBD make the volume of the ERβ binding pocket somewhat smaller than that of ERα, and this is one of the aspects that may be exploited to design ERβ-selective ligands.

We have recently reported selective ERβ agonists[10] characterized by a monoaryl-substituted salicylketoxime scaffold, which showed an improved binding affinity and selectivity compared to those of their aldoxime analogs.[11] In the previous chemical exploration of the salicylketoxime class, we inserted small, open-chain lipophilic alkyl groups (methyl, ethyl or trifluoromethyl group) in the ketoxime moiety (*A*, Figure 1), since they provided groups suitable to fill the hydrophobic cavity identified by our modeling studies. In order to develop this class of derivatives further, we planned to introduce a five-membered cyclic alkyl group (*B*, Figure 1) fused onto the central phenolic ring, in the hope that they would produce compounds with improved binding affinity and selectivity for ERβ. The newly synthesized derivatives (**1a–i**, Figure 1) differ in terms of the substituents on the aryl ring (R^1 and R^2); the presence of a *para*-OH group on the peripheral phenyl ring was maintained (compound **1a**, Figure 1), in consideration of the encouraging results obtained with this substituent in the previous class of salycilketoximes.[10] Moreover, we investigated whether the addition of an extra substituent (F, CH_3, Cl, compounds **1c**, **e** and **g**, Figure 1) in the *meta* position could be beneficial for the activity and selectivity of the resulting compounds. Then, the *O*-methylated analogs of compounds **1a**, **c**, **e** and **g** were synthesized to determine the effect of the replacement of the phenolic hydroxyl by a group that can only act as a hydrogen-bond acceptor (compounds **1b**, **d**, **f**, **h**, Figure 1). Finally, the removal of the 4-OH group was also done to assess the importance of this group for binding to the receptor (compound **1i**, Figure 1).

Results and Discussion

Chemistry

The synthesis of salicylketoximes starts from commercially available 4-bromo-7-hydroxy-1-indanone **2**, which was subjected to a palladium-catalyzed cross-coupling reaction under classical Suzuki conditions, with the properly substituted arylboronic acids, to obtain biaryl compounds **3b**, **3d**, **3f**, **3h** and **3i** (Scheme 1). In particular, the bromo-aryl derivative was reacted with a slight excess of arylboronic acid in the presence of tetrakis(triphenylphosphine)palladium as the *in situ*-formed catalyst, in a solvent mixture of toluene and ethanol and in the presence of aqueous sodium carbonate as the base, under conventional heating at 100 °C.

Hydroxy-substituted intermediates **3a**, **3c**, **3e** and **3g**, were obtained by treatment of the corresponding methoxy-substituted biaryl ketones **3b**, **3d**, **3f**, **3h** with boron tribromide. Finally, reaction of the cyclic ketone precursors with hydroxylamine hydrochloride produced the final compounds **1a–i**.

As we previously observed for structurally similar salicylketoxime derivatives,[10, 12] cyclic ketoximes **1a–i** showed the *E*-configuration in their oxime portion.[13] Analysis of the ^{1}H-NMR spectra revealed that the chemical shift values (δ) of the ketoximic methylenic protons in position α to the oxime group are in agreement with those reported in the literature for the *E*-isomers of similar methyl-ketoxime derivatives ($2.83 \leq \delta \leq 2.96$ ppm). This observation can be explained considering that the *E*-diastereoisomer is stabilized by the highly energetic intramolecular H-bond between the phenolic OH group and the nearby nitrogen atom of the oxime portion.

Biological Evaluation

Ligand Binding Affinity—The binding affinity of ketoximes **1a–i** for ERα and ERβ was measured by a radiometric competitive binding assay, using previously reported methods.[14] The relative binding affinity (RBA) values for the newly reported compounds are summarized in Table 1. RBA values are reported as percentage (%) of that of estradiol (E_2), which is set at 100%.

The presence of the *para*-OH group on the distal phenyl ring in compound **1a** produced good binding to the β isoform (RBA = 4.28%, K_i = 11.7 nM), also accompanied by a reduced affinity for ERα, resulting in a good degree of selectivity for ERβ (β/α ratio = 16). A slight improvement was produced when a *m*-fluorine atom was introduced in the aryl substituent (**1c**): good affinity for ERβ was substantially preserved (RBA = 4.71%, K_i = 10.6 nM), and a certain loss of binding to ERα was observed, thus resulting in an enhanced ERβ selectivity (β/α ratio = 33). Conversely, the insertion of an additional substituent such as a *m*-chlorine atom (**1g**) or a *m*-methyl group (**1e**) into the 4-hydroxyphenyl group resulted in a severe reduction of the binding to ERβ and a compromised ERβ subtype selectivity. The *O*-methylated analogs (**1b**, **1d**, **1f**, **1h**) displayed a dramatic loss of affinity for both receptors. The binding values of unsubstituted ketoxime **1i** show a modest affinity (24-fold decrease compared to **1a**) but an excellent selectivity for ERβ (β/α ratio = 89).

Fluorescence-Based Coactivator Interaction Assays—The three compounds (**1a**, **1c** and **1i**) showing the best profile in terms of affinity and selectivity were submitted to *in vitro* time resolved-fluorescence resonance energy transfer (tr-FRET) functional assays to test their ability to form active complexes with ERs, that is, those which are able to recruit coactivators. Estradiol was always used as the reference receptor activator. Transcriptional activity assays conducted in tissue culture cells containing either ERα or ERβ receptors have long been used to probe structure/function activity of new ligands. Reporter gene transfection assays can be conducted in human endometrial (HEC-1) cells (which express nuclear receptor coactivators, but contain no endogenous ERs), using introduced expression plasmids for full-length human ERs and an estrogen-responsive luciferase reporter gene system.[15] These experiments require the laboratory to be equipped to grow and maintain tissue culture cells, a large expense in terms of equipment and growth media, as well as in researcher time to comply with government regulations and to maintain the cells.

A simple, alternative to the intracellular tissue culture assay is a cell-free, fluorescence-based assay for coactivator recruitment using purified ER-LBDs and a coactivator labeled

with suitable fluorophores. The use of a tr-FRET assay [16, 17] of this design is very useful to quantitatively probe the ability of new ligands to form a complex with the ER that is capable of recruiting coactivator, an important indicator of an active biological complex. This assay can be performed in two ways: coactivator titration into a preformed ER-ligand complex measures the affinity of the coactivator. By contrast, ligand titration into a fixed concentration of ER and coactivator mimics the results of the more traditional CARLA (coactivator-dependent receptor ligand assay) assay,[18, 19] and is a measure of ligand potency in terms of coactivator recruitment. These assays can also distinguish agonist ligands from antagonist ligands. In essence, these *in vitro* assays act as a surrogate measure for the process that takes place in target cells, and the results obtained using these *in vitro* coactivator recruitment assays show a remarkable correlation with potency measurements obtained from cell-based assays.[20]

Assay of Coactivator Binding Affinity—Initially, the steroid receptor coactivator-3 (SRC3) was titrated into 1 nM of ER ligand binding domain (LBD) site-specifically bound with biotin and with 0.25 nM streptavidin-terbium (SaTb), ERα LBD/C417-biotin and ERβ LBD/C369-biotin bound with 1 μM of the ligand. To this were added increasing amounts of SRC3 nuclear receptor interaction domain (NRID) labeled with fluorescein, SRC3 NRID-fluorescein.[20, 21] The formation of ER-estrogen-coactivator complexes was measured by quantifying the increase in the tr-FRET signal as a function of increasing SRC concentration, from which an EC_{50} value, representing the affinity of SRC3 for the ER-ligand complex, could be obtained. All curves are corrected for the background of diffusion-enhanced FRET. The results (Figure 2 and Table 2) show a concentration dependent and ligand-specific increase in tr-FRET signal upon SRC3 binding to ERβ. In this experiment, the cyclic ketoximes formed complexes with ERβ to which SRC3 bound well; this was particularly the case with compounds **1a** and **1c**, and to a lesser extent, **1i**. Also, the completeness of the curves for **1a** and **1c** is nearly as high as that of E_2 (93 and 88%, respectively, Table 3), while that of **1i** is lower (72%), suggesting that the last compound might have a somewhat lower agonist efficacy or intrinsic activity. None of the tested ligands enable SRC3 to bind to ERα, consistent with their low affinity binding to this subtype. By contrast, with estradiol there is a nice increase in tr-FRET upon SRC3 binding to both ERα and ERβ. ERα is unable to recruit SRC in the absence of agonist ligand (Figure 2, upper part). ERβ, however, is able to recruit SRC to some degree, even in the apo state (see open circles in the ERβ graph of Figure 2), consistent with the low constitutive activity shown by this ER subtype.

Assay of Ligand Potency in Coactivator Recruitment—As a measure of estrogen potency, we titrated the ligands into a constant amount of 1 nM ERβ/C369-biotin-SaTb and 100 nM SRC3 NRID-fluorescein. Since there was no SRC recruitment to ERα, the ligand titration with ERα was not performed. It is evident from the graph (Figure 3) that the ligands have the same order of recruitment to ERβ as they have affinity for this ER subtype. Table 3 contains a quantitative summary of SRC3 binding affinities (as EC_{50} values), ligand coactivator recruitment potencies (as EC_{50} values), and ligand binding affinities (RBA values, also converted to K_i values). As expected, the ligand coactivator recruitment potencies and ligand binding affinities (K_i values) are remarkably similar, being,

respectively, an indirect and a direct measure of ligand affinity. The EC_{50} values that represent the binding affinities of SRC3 to the ERβ-ligand complexes, by contrast, cover a much smaller range, which reflects the fact all three of these ketoxime ligands are expected to have a good level of agonist efficacy.

Antiproliferative assays—The most potent ERβ agonists among cyclic ketoximes were evaluated for their ability to block cell proliferation, in comparison with the reference ERβ agonist liquiritigenin, a natural flavone that is a major component in licorice root extracts. Compounds **1a**, **1c** and liquiritigenin were screened on a series of cancer cell lines such as glioma (U87), colon (LoVo, HCT), and breast (MDA-MB-231, MCF7, SkBr3) cancer cells (Table 4). As we have previously reported,[10] ERβ is known to exert an antiproliferative effect in glioma, colorectal and breast tumors. Moreover, we included in our study the ERβ negative breast cancer cell line SkBr3 in order to verify the contribution of ERβ activation to the antiproliferative effect of these compounds. In all ERβ-positive cell lines, ketoxime derivatives **1a** and **1c** displayed the most potent inhibition of proliferation when compared to liquiritigenin. Notably, the activities of **1a** and **1c** against SkBr3 cells were significantly lower than their activities against all the other ERβ-positive cancer cells, and these compounds proved to be more selective than liquiritigenin for ERβ-containing cells. If we limit our comparison only to breast cancer cells, in order to better evaluate the involvement of ERβ in the antiproliferative effect displayed by these two compounds, we can observe that the IC_{50} values found in ERβ-positive MDA231 and MCF7 cells (from 8.1 to 70.1 μM) are 2- to 16-fold lower than those in ERβ-negative SkBr3 cells (130.4–139.9 μM). However, we cannot exclude the involvement of other mechanisms in the inhibition of proliferation by compounds **1a** and **1c,** since a certain degree of inhibition is also observed in SkBr3 cells. Overall, compound **1c**, which showed the highest ERβ binding affinity and selectivity, proved to be the most potent antiproliferative agent in these cell lines.

Molecular Modeling and design

In order to suggest a possible binding mode for this class of derivatives, the interaction of compound **1a** into ERβ was analyzed by means of docking and molecular dynamic (MD) simulations. As shown in Figure 4, the docking results suggest two different possible binding orientations for this compound. In both cases the pseudocycle oxime system forms an H-bond with E305, and the bicyclic scaffold establishes lipophilic interactions with A302, M336, and F356.

In binding orientation A (Figure 4), the phenolic OH group forms an H-bond with H475, whereas in the binding orientation B (Figure 4) the phenol ring points towards T299, showing an H-bond with the hydroxyl group of this residue.

The two complexes were then subjected to 100 ns of MD simulation with explicit water molecules, as described in the Experimental section. Figure S1 in the Supporting Information shows the MD analysis for the binding orientation A of compound **1a** into ERβ. After about 2 ns of MD, the system reached an equilibrium, since the total energy for the last 98 ns remained approximately constant. Analyzing the root-mean-square deviation (RMSD) of all the α carbons of the protein from the starting ERβ structure, we observed that after an

initial increase, in the last 75 ns the RMSD remained stable around the value of 2.0 Å. Furthermore, as shown in Figure 5, the two interactions with E305 and H475 displayed a good stability as they were maintained for more than 75% of the MD simulation.

Figure 6 shows the analysis of the MD trajectory for the binding mode B of compound **1a** into ERβ. The H-bond interaction between the pseudocycle/oxime system and E305 was stable during the whole MD simulation. With regards to the H-bond between the phenolic oxygen and T299, it was maintained only during about the first 20 ns of the MD simulation, whereas in the remaining 80 ns the ligand switched from binding mode B to binding mode A, forming a stable H-bond with H475. On the basis of these MD results, binding mode A should be considered the more reliable. Furthermore, this binding pose is also in agreement with the reported SAR analysis that indicates a key role for the H-bond donor properties of the phenolic OH group of this class of compounds (see poor ERβ-binding affinities of compounds **1b**, **1d**, **1f**, **1h**). In fact, while T299 is able to act as both an H-bond donor and acceptor, thus being potentially able to establish attractive interactions with H-bond donating/accepting groups, H475 mainly act as a H-bond acceptor in ER binding cavities. This consideration is supported by the elevated ERβ-binding affinities displayed by compounds possessing 4-hydroxyaryl substituents, such as **1a**, **1c**, **1e**, **1g**, when compared to those measured for the rest of the series.

In order to verify whether compound **1a** is able to maintain in ERα the same binding orientation and interactions displayed in ERβ, a complex of ERα with the binding orientation A of compound **1a** was generated and subjected to 100 ns of MD simulation in the condition reported above.

Figure 7 shows the average minimized structure of the ERα-**1a** complex obtained from the MD simulation. This compound was able to maintain the H-bond with H524 by means of its phenolic OH group, but its pseudocycle/oxime system was not able to interact efficiently with E305, and in addition, it did not show any other important interactions, thereby being consistent with its low binding affinity for this receptor subtype. These results were also confirmed by analyzing the behavior of the two H-bond interactions during the whole MD simulation. As shown in Figure S2 in the Supporting Information the interaction of the phenolic hydroxyl with H524 was conserved for more than 75% of the MD simulation, whereas the interaction of the pseudocycle/oxime system with E305 was maintained only for about 35% of the simulation.

The MD trajectories obtained for both ERα and ERβ were also further analyzed through the MM-PBSA method,[22] which can be used to estimate the ligand–receptor energy interaction.[12, 23] This approach averages the contributions of gas phase energies and solvation free energies calculated for snapshots of the complex molecule as well as the unbound components extracted from MD trajectories, according to the procedure fully described in the Supporting Information. The MM-PBSA results (Supporting Information, Table S1) suggested that the interaction of the ligand with the ERβ-binding cavity was more stable of about 6 kcal•mol^{-1} with respect to its interaction with ERα, consistent with the observed ERβ selectivity of compound **1a**.

Conclusions

In summary, we have designed and synthesized a new class of cyclic salicylketoximes, by the introduction of a new five-membered condensed cyclic portion, which was identified as a suitable moiety to fill a small hydrophobic pocket present in ERβ-binding cavity. This chemical modification was explored to see whether the enlargement from the previous small open-chain alkyl groups to this alkyl cycle could be tolerated by the ERβ-ligand cavity. These compounds proved able to bind with good affinity and selectivity to ERβ. In particular, the presence of the *para*-hydroxy substituted peripheral phenyl ring increases the potency of the ligands, and modeling studies confirmed the key role of this phenolic group in the binding disposition of this series of compounds. Moreover, cell-free coactivator recruitment assays were used to assess the functional properties of these compounds, which showed them to be potent and selective ERβ-agonists. Furthermore, this functional assay highlighted a significant parallel trend with the results observed in the receptor binding assays. Finally, the most potent ERβ-agonists also proved to efficiently inhibit cell proliferation in ERβ-positive cancer cell lines.

Experimental Section

General Procedures and Materials

All solvents and chemicals were used as purchased without further purification. Chromatographic separations were performed on silica gel columns by flash chromatography (Kieselgel 40, 0.040–0.063 mm; Merck). Reactions were followed by thin layer chromatography (TLC) on Merck aluminum silica gel (60 F254) sheets that were visualized under a UV lamp. Evaporation was performed in vacuo (rotating evaporator). Sodium sulfate was always used as the drying agent. Proton (^{1}H) and carbon (^{13}C) NMR spectra were obtained with a Bruker Avance III 400 MHz spectrometer using the indicated deuterated solvents. Chemical shifts are given in parts per million (ppm) (δ relative to residual solvent peak for ^{1}H and ^{13}C). High-resolution mass spectrometry (HRMS) analysis was performed using a Waters Quattro II quadrupole–hexapole–quadrupole liquid chromatography/mass spectrometry apparatus (Waters, Milford, MA) equipped with an electrospray ionization source. Yields refer to isolated and purified products derived from non-optimized procedures.

Preparation of cyclic ketones 3b, d, f, h, i

General procedure—A solution of $Pd(OAc)_2$ (0.02 eq) and triphenylphosphine (0.1 eq) in ethanol (0.64 mL/0.66 mmol compound **2**) and toluene (0.64 mL/0.66 mmol compound **2**) was stirred at RT under nitrogen for 10 min. After that period, compound **2** (1 eq), 0.66 mL of an aqueous 2 M solution of Na_2CO_3, and the properly substituted arylboronic acid (1.3 eq) were sequentially added. The resulting mixture was heated at 100 °C in a sealed vial under nitrogen for 24 h. After being cooled to RT, the mixture was diluted with water and extracted with EtOAc. The combined organic phase were dried and concentrated. The crude product was purified by flash chromatography by eluting with *n*-hexane/EtOAc (95:5 to 9:1) affording the desired ketone intermediates.

7-Hydroxy-4-(4-methoxyphenyl)-2,3-dihydro-1*H*-inden-1-one (3b): (81% yield from **2**) ^{1}H NMR (400 MHz, $CDCl_3$): δ = 2.73 (t, *J* = 5.7 Hz, 2H), 3.16 (t, *J* = 5.7 Hz, 2H), 3.86 (s, 3H), 6.85 (d, *J* = 8.3 Hz, 1H), 6.95–7.00 (m, 2H), 7.32–7.36 (m, 2H), 7.48 (d, *J* = 8.4 Hz, 1H), 9.28 ppm (*exchangeable* s, 1H).

4-(3-Fluoro-4-methoxyphenyl)-7-hydroxy-2,3-dihydro-1*H*-inden-1-one (3d): (78% yield from **2**) ^{1}H NMR (400 MHz, $CDCl_3$): δ = 2.72–2.75 (m, 2H), 3.16 (t, *J* = 5.7 Hz, 2H), 3.94 (s, 3H), 6.86 (d, *J* = 8.4 Hz, 1H), 7.03 (t, *J* = 8.5 Hz, 1H), 7.12 (ddd, *J* = 8.3, 2.2, 1.0 Hz, 1H), 7.16 (dd, *J* = 12.2, 2.0 Hz, 1H), 7.47 (d, *J* = 8.4 Hz, 1H), 9.31 ppm (*exchangeable* s, 1H).

7-Hydroxy-4-(4-methoxy-3-methylphenyl)-2,3-dihydro-1*H*-inden-1-one (3f): (81% yield from **2**) ^{1}H NMR (400 MHz, $CDCl_3$): δ = 2.27 (s, 3H), 2.71–2.74 (m, 2H), 3.17 (t, *J* = 5.6 Hz, 2H), 3.88 (s, 3H), 6.84 (d, *J* = 8.3 Hz, 1H), 6.89 (d, *J* = 8.1 Hz, 1H), 7.18–7.23 (m, 2H), 7.48 (d, *J* = 8.4, 1H), 9.27 ppm (*exchangeable* s, 1H).

4-(3-Chloro-4-methoxyphenyl)-7-hydroxy-2,3-dihydro-1*H*-inden-1-one (3h): (88% yield from **2**) ^{1}H NMR (400 MHz, [D_6]acetone): δ = 2.71–2.75 (m, 2H), 3.22 (t, *J* = 5.5 Hz, 2H), 3.96 (s, 3H), 6.85 (d, *J* = 8.3 Hz, 1H), 7.22 (d, *J* = 8.5 Hz, 1H), 7.45 (dd, *J* = 8.5, 2.2 Hz, 1H), 7.53 (d, *J* = 2.2 Hz, 1H), 7.56 (d, *J* = 8.4 Hz, 1H), 9.39 ppm (*exchangeable* bs, 1H).

7-Hydroxy-4-phenyl-2,3-dihydro-1*H*-inden-1-one (3i): (76% yield from **2**) ^{1}H NMR (400 MHz, $CDCl_3$): δ = 2.72–2.75 (m, 2H), 3.18 (t, *J* = 5.7 Hz, 2H), 6.88 (d, *J* = 8.3 Hz, 1H), 7.34–7.48 (m, 5H), 7.52 (d, *J* = 8.4 Hz, 1H), 9.32 ppm (*exchangeable* s, 1H).

Preparation of *O*-deprotected cyclic ketones 3a, c, e, g

General Procedure—A solution of pure ketones **3b, d, f, h** (0.32 mmol) in anhydrous CH_2Cl_2 (3.7 mL) was cooled to −78 °C and treated dropwise with a 1.0 M solution of BBr_3 in CH_2Cl_2 (1.0 mL) under nitrogen. The mixture was left under stirring at the same temperature for 5 min and then at 0 °C for 1 h. The mixture was then diluted with water and extracted with EtOAc. The organic phase was dried and concentrated. The crude product was purified by flash chromatography over silica gel. Elution with *n*-hexane/EtOAc (8:2) afforded the desired *O*-deprotected ketones.

7-Hydroxy-4-(4-hydroxyphenyl)-2,3-dihydro-1*H*-inden-1-one (3a): (85% yield from **3b**) ^{1}H NMR (400 MHz, [D_6]acetone): δ = 2.70–2.73 (m, 2H), 3.19 (t, *J* = 5.7 Hz, 2H), 6.82 (d, *J* = 8.3 Hz, 1H), 6.94 (AA′XX′, J_{AX} = 8.8 Hz, $J_{AA'/XX'}$ = 2.5 Hz, 2H), 7.35 (AA′XX′, J_{AX} = 8.7 Hz, $J_{AA'/XX'}$ = 2.5 Hz, 2H), 7.52 (d, *J* = 8.3 Hz, 1H), 8.47 (*exchangeable* bs, 1H), 9.34 ppm (*exchangeable* bs, 1H).

4-(3-Fluoro-4-hydroxyphenyl)-7-hydroxy-2,3-dihydro-1*H*-inden-1-one (3c): (79% yield from **3d**) ^{1}H NMR (400 MHz, [D_6]acetone): δ = 2.71–2.75 (m, 2H), 3.22 (t, *J* = 5.5 Hz, 2H,), 6.84 (d, *J* = 8.3 Hz, 1H), 7.09 (t, *J* = 8.7 Hz, 1H), 7.18 (ddd, *J* = 8.3, 2.1, 0.9 Hz, 1H), 7.27 (dd, *J* = 12.3, 2.1 Hz, 1H), 7.56 ppm (d, *J* = 8.4 Hz, 1H).

7-Hydroxy-4-(4-hydroxy-3-methylphenyl)-2,3-dihydro-1H-inden-1-one (3e): (89% yield from **3f**) ^{1}H NMR (400 MHz, [D$_6$]acetone): δ = 2.26 (s, 3H), 2.68–2.73 (m, 2H), 3.20 (t, *J* = 5.6 Hz, 2H), 6.82 (d, *J* = 8.3 Hz, 1H), 6.91 (d, *J* = 8.2 Hz, 1H), 7.16 (dd, *J* = 8.2, 2.4 Hz, 1H), 7.24 (d, *J* = 1.9 Hz, 1H), 7.51 (d, *J* = 8.3 Hz, 1H), 8.31 (*exchangeable* bs, 1H), 9.33 ppm (*exchangeable* bs, 1H).

4-(3-Chloro-4-hydroxyphenyl)-7-hydroxy-2,3-dihydro-1*H*-inden-1-one (3g): (90% yield from **3h**) ^{1}H NMR (400 MHz, [D$_6$]acetone): δ = 2.70–2.74 (m, 2H), 3.22 (t, *J* = 5.5 Hz, 2H), 6.84 (d, *J* = 8.3 Hz, 1H), 7.11 (d, *J* = 8.4 Hz, 1H), 7.33 (dd, *J* = 8.4, 2.2 Hz, 1H), 7.48 (d, *J* = 2.2 Hz, 1H), 7.55 (d, *J* = 8.4 Hz, 1H), 9.10 ppm (*exchangeable* bs, 1H).

Preparation of Final Products 1a–i

General Procedure—A solution of pure ketones **3a–i** (1 eq) in ethanol (3.8 mL/0.20 mmol ketone) was treated with a solution of hydroxylamine hydrochloride (2 eq) in water (0.9 mL/0.40 mmol $NH_2OH{\cdot}HCl$), and the mixture was heated to 50 °C for 24 h. After being cooled to RT, part of the solvent was removed under vacuum, and the mixture was diluted with water and extracted with EtOAc. The organic phase was dried and evaporated to afford a crude residue that was purified by column chromatography (*n*-hexane/EtOAc 95:5 to 7:3) to afford the desired cyclic ketoxime derivatives.

(*E*)-7-hydroxy-4-(4-hydroxyphenyl)-2,3-dihydro-1*H*-inden-1-one oxime (1a): Off-white solid; yield 83% from **3a**. ^{1}H-NMR (400 MHz, [D$_6$]DMSO): δ = 2.83 (t, *J* = 6.5 Hz, 2H), 3.06 (t, *J* = 6.4 Hz, 2H), 6.76–6.84 (m, 3H), 7.17 (d, *J* = 8.3 Hz, 1H), 7.25 (AA′XX′, J_{AX} = 8.6 Hz, $J_{AA'/XX'}$ = 2.4 Hz, 2H), 8.98 (*exchangeable* bs, 1H), 9.46 ppm (*exchangeable* bs, 1H), 11.06 (*exchangeable* bs, 1H); ^{13}C-NMR (100 MHz, [D$_6$]DMSO): δ = 25.8, 28.5, 113.4, 115.2 (2C), 122.0, 129.1 (2C), 130.2, 130.2, 131.0, 145.8, 152.8, 156.3, 164.4. HRMS-ESI m/z $[M+H]^+$ calcd for $C_{15}H_{13}NO_3$: 256.0974, found: 256.0963.

(*E*)-7-hydroxy-4-(4-methoxyphenyl)-2,3-dihydro-1*H*-inden-1-one oxime (1b): Off-white solid; yield 57% from **3b**. ^{1}H-NMR (400 MHz, [D$_6$]DMSO): δ = 2.83 (t, *J* = 6.4 Hz, 2H), 3.07 (t, *J* = 6.3 Hz, 2H), 3.78 (s, 3H), 6.80 (d, *J* = 8.2 Hz, 1H), 6.96–7.01 (m, 2H), 7.20 (d, *J* = 8.2 Hz, 1H), 7.35–7.41 (m, 2H), 9.02 (*exchangeable* s, 1H), 11.08 ppm (*exchangeable* s, 1H); ^{13}C-NMR (100 MHz, [D$_6$]DMSO): δ = 25.8, 28.5, 55.1, 113.5, 113.9 (2C), 122.0, 129.2 (2C), 129.8, 131.1, 131.9, 145.9, 153.0, 158.2, 164.3. HRMS-ESI m/z $[M+H]^+$ calcd for $C_{16}H_{15}NO_3$: 270.1130, found: 270.1120.

(*E*)-4-(3-fluoro-4-hydroxyphenyl)-7-hydroxy-2,3-dihydro-1*H*-inden-1-one oxime (1c): Light-yellow solid; yield 70% from **3c**. ^{1}H-NMR (400 MHz, [D$_6$]acetone): δ = 2.94–2.97 (m, 2H), 3.17 (t, *J* = 6.4 Hz, 2H), 6.79 (d, *J* = 8.3 Hz, 1H), 7.06 (t, *J* = 8.7 Hz, 1H), 7.13 (ddd, *J* = 8.4, 2.1, 0.7 Hz, 1H), 7.21 (dd, *J* = 12.3, 2.1 Hz, 1H), 7.25 (d, *J* = 8.3 Hz, 1H), 8.68 (*exchangeable* bs, 1H), 8.77 (*exchangeable* s, 1H), 10.26 ppm (*exchangeable* bs, 1H); ^{13}C-NMR (100 MHz, [D$_6$]acetone): δ = 26.5, 29.6, 114.4, 116.6 (d, *J* = 19.1 Hz), 118.7 (d, *J* = 3.0 Hz), 123.0, 125.4 (d, *J* = 3.0 Hz), 130.4, 132.5, 133.2 (d, *J* = 6.0 Hz), 144.6 (d, *J* = 14.1 Hz), 147.0, 152.2 (d, *J* = 240.5 Hz), 155.0, 166.4. HRMS-ESI m/z $[M+H]^+$ calcd for $C_{15}H_{12}FNO_3$: 274.0879, found: 274.0867.

(*E*)-4-(3-fluoro-4-methoxyphenyl)-7-hydroxy-2,3-dihydro-1*H*-inden-1-one oxime (1d): Light-yellow solid; yield 44% from **3d**. ^{1}H-NMR (400 MHz, [D$_6$]acetone): δ = 2.94–2.98 (m, 2H), 3.17 (t, *J* = 6.5 Hz, 2H), 3.92 (s, 3H), 6.80 (d, *J* = 8.4 Hz, 1H), 7.19 (t, *J* = 8.5 Hz, 1H), 7.22–7.28 (m, 3H), 8.79 (*exchangeable* s, 1H), 10.28 ppm (*exchangeable* s, 1H); ^{13}C-NMR (100 MHz, [D$_6$]acetone): δ = 25.2, 29.6, 56.6, 114.5 (d, *J* = 18.1 Hz), 114.6, 116.6 (d, *J* = 18.1 Hz), 123.0, 125.2 (d, *J* = 3.0 Hz), 130.2, 132.5, 134.0 (d, *J* = 6.0 Hz), 147.1, 147.5 (d, *J* = 10.1 Hz), 152.9 (d, *J* = 244.5 Hz), 155.1, 166.4. HRMS-ESI m/z [M+H]$^+$ calcd for $C_{16}H_{14}FNO_3$: 288.1036, found: 288.1028.

(*E*)-7-hydroxy-4-(4-hydroxy-3-methylphenyl)-2,3-dihydro-1*H*-inden-1-one oxime (1e): Light-orange solid; yield 41% from **3e**. ^{1}H-NMR (400 MHz, [D$_6$]acetone): δ = 2.25 (s, 3H), 2.92–2.96 (m, 2H), 3.14 (t, *J* = 6.4 Hz, 2H), 6.76 (d, *J* = 8.3 Hz, 1H), 6.88 (d, *J* = 8.2 Hz, 1H), 7.11 (dd, *J* = 8.2, 2.3 Hz, 1H), 7.18–7.23 (m, 2H), 8.25 (*exchangeable* s, 1H), 8.71 (*exchangeable* s, 1H), 10.23 ppm (*exchangeable* s, 1H); ^{13}C-NMR (100 MHz, [D$_6$]acetone): δ = 16.3, 26.5, 30.1, 114.1, 115.5, 122.8, 125.0, 127.5, 131.6, 131.8, 132.2, 132.4, 146.7, 154.5, 155.3, 166.6. HRMS-ESI m/z [M+H]$^+$ calcd for $C_{16}H_{15}NO_3$: 270.1130, found: 270.1125.

(*E*)-7-hydroxy-4-(4-methoxy-3-methylphenyl)-2,3-dihydro-1*H*-inden-1-one oxime (1f): Yellow solid; yield 89% from **3f**. ^{1}H-NMR (400 MHz, [D$_6$]acetone): δ = 2.22 (s, 3H), 2.92–2.96 (m, 2H), 3.15 (t, *J* = 6.4 Hz, 2H), 3.87 (s, 3H), 6.78 (d, *J* = 8.3 Hz, 1H), 6.97 (d, *J* = 8.6 Hz, 1H), 7.21–7.27 (m, 3H), 8.73 (*exchangeable* s, 1H), 10.24 ppm (*exchangeable* s, 1H); ^{13}C-NMR (100 MHz, [D$_6$]acetone): δ = 16.4, 26.5, 30.1, 55.7, 110.9, 114.2, 122.9, 126.9, 127.6, 131.3, 131.6, 132.5, 133.0, 147.0, 154.7, 157.8, 166.5. HRMS-ESI m/z [M+H]$^+$ calcd for $C_{17}H_{17}NO_3$: 284.1287, found: 284.1273.

(*E*)-4-(3-chloro-4-hydroxyphenyl)-7-hydroxy-2,3-dihydro-1*H*-inden-1-one oxime (1g): Yellow solid; yield 63% from **3g**. ^{1}H-NMR (400 MHz, [D$_6$]acetone): δ = 2.94–2.97 (m, 2H), 3.16 (t, *J* = 6.4 Hz, 2H), 6.79 (d, *J* = 8.4 Hz, 1H), 7.08 (d, *J* = 8.4 Hz, 1H), 7.24 (d, *J* = 8.3 Hz, 1H), 7.27 (dd, *J* = 8.4, 2.2 Hz, 1H), 7.43 (d, *J* = 2.2 Hz, 1H), 8.77 ppm (*exchangeable* bs, 1H); ^{13}C-NMR (100 MHz, [D$_6$]acetone): δ = 26.5, 29.5, 114.4, 117.6, 121.1, 123.0, 128.9, 130.2, 130.3, 132.4, 133.7, 147.0, 152.8, 155.0, 166.4. HRMS-ESI m/z [M+H]$^+$ calcd for $C_{15}H_{12}ClNO_3$: 290.0584, found: 290.0572.

(*E*)-4-(3-chloro-4-methoxyphenyl)-7-hydroxy-2,3-dihydro-1*H*-inden-1-one oxime (1h): Yellow solid; yield 19% from **3h**. ^{1}H-NMR (400 MHz, [D$_6$]acetone): δ = 2.94–2.98 (m, 2H), 3.16 (t, *J* = 6.4 Hz, 2H), 3.94 (s, 3H), 6.80 (d, *J* = 8.3 Hz, 1H), 7.18 (d, *J* = 8.5 Hz, 1H), 7.26 (d, *J* = 8.3 Hz, 1H), 7.40 (dd, *J* = 8.5, 2.2 Hz, 1H), 7.48 (d, *J* = 2.2 Hz, 1H), 8.79 (*exchangeable* s, 1H), 10.30 ppm (*exchangeable* s, 1H); ^{13}C-NMR (100 MHz, [D$_6$]acetone): δ = 26.5, 29.5, 56.6, 113.4, 114.4, 122.7, 123.1, 128.8, 123.0, 130.5, 132.5, 134.4, 147.1, 154.9, 155.1, 166.4. HRMS-ESI m/z [M+H]$^+$ calcd for $C_{16}H_{14}ClNO_3$: 304.0740, found: 304.0732.

(*E*)-7-hydroxy-4-phenyl-2,3-dihydro-1*H*-inden-1-one oxime (1i): Off-white solid; yield 67% from **3i**. ^{1}H-NMR (400 MHz, [D$_6$]acetone): δ = 2.94– 2.98 (m, 2H), 3.16 (t, *J* = 6.4

Hz, 2H), 6.82 (d, *J* = 8.3 Hz, 1H), 7.28 (d, *J* = 8.3 Hz, 1H), 7.33 (tt, *J* = 7.0, 1.9 Hz, 1H), 7.41–7.49 (m, 4H), 8.79 (*exchangeable* s, 1H), 10.28 ppm (*exchangeable* s, 1H); ^{13}C-NMR (100 MHz, [D_6]acetone): δ = 26.5, 29.6, 114.4, 123.0, 127.6, 129.1 (2C), 129.3 (2C), 131.6, 132.6, 141.0, 147.1, 155.1, 166.4. HRMS-ESI m/z $[M+H]^+$ calcd for $C_{15}H_{13}NO_2$: 240.1025, found: 240.1016.

Modeling

Docking of compound 1a—The crystal structure of ERα (PDB code 2I0J) and ERβ (PDB code 2I0G),[24] was taken from the Protein Data Bank.[25] The ligand was built using Maestro, version 9.0 (Schrödinger Inc: Portland, OR, 2009) and was subjected to a conformational search (CS) of 1000 steps, using a water environment model (generalized-Born/surface-area model) by means of Macromodel, version 9.7 (Schrödinger Inc: Portland, OR, 2009). The algorithm used was based on the Monte Carlo method with the MMFFs force field and a distance-dependent dielectric constant of 1.0. The ligand was then energy minimized using the conjugated gradient method until a convergence value of 0.05 kcal/(Å•mol) was reached, using the same force field and parameters used for the CS. Automated docking was carried out by means of the Autodock 4.0 program.[26] AUTODOCK Tools utilities[27] were used in order to identify the torsion angles in the ligands, to add the solvent model and assign the Gasteiger atomic charges to protein and ligands. The regions of interest used by AUTODOCK were defined by considering SERBA-1 as the central group of a grid box of 10 Å in the x, y, and z directions. A grid spacing of 0.375 Å and a distance dependent function of the dielectric constant were used for the energetic map calculations. By using the Lamarckian genetic algorithm, the docked compounds were subjected to 100 runs of the AUTODOCK search using 2,500,000 steps of energy evaluation and the default values of the other parameters. The resulting docking poses were clustered using a threshold of 2.0 Å and for each cluster one representative docking pose was subjected to MD simulation.

MD simulations—All simulations were performed using AMBER 14.[28] MD simulations were carried out using the parm10 force field at 300 K. The complexes were placed in a rectangular parallelepiped water box. An explicit solvent model for water, TIP3P, was used, and the complexes were solvated with a 15 Å water cap. Sodium ions were added as counterions to neutralize the system. Prior to MD simulations, two steps of energy minimization were carried out. In the first stage, we kept the protein and ligand fixed with a position restraint of 100 kcal/(mol•Å^2) and we just energy minimized the positions of the water molecules. In the second stage, we applied a restraint of 30 kcal/(mol•Å^2) only on the α carbons of the receptor. The two energy minimization stages consisted of 10,000 steps. The first 1000 steps were steepest descent, and the last 9000 were conjugate gradient. Molecular dynamics trajectories were run using the energy minimized structure as the input, and particle mesh Ewald electrostatics[29] and periodic boundary conditions were used in the simulation. The time step of the simulations was 2.0 fs with a cutoff of 12 Å for the non-bonded interaction. SHAKE was employed to keep all bonds involving hydrogen atoms rigid. Constant-volume periodic boundary MD was carried out for 500 ps, during which the temperature was raised from 0 to 300 K. Then 99.5 ns of constant pressure periodic boundary MD was carried out at 300 K using the Langevin thermostat to maintain constant

the temperature of our system. General Amber force field (GAFF) parameters were assigned to the ligand, while partial charges were calculated using the AM1-BCC method as implemented in the Antechamber suite of AMBER 14.

Energy evaluation—We extracted from the last 50 ns of MD of the ligand-receptor complexes, 100 snapshots (at time intervals of 500 ps) for each species (complex, receptor and ligand). Electrostatic, van der Waals and internal energies were obtained using the SANDER module in AMBER 14. Polar energies were obtained from the PBSA module of the AMBER 14 program (using the Poisson-Boltzman method) applying dielectric constants of 1 and 80 to represent the gas and water phases, respectively. Nonpolar energies were determined using the MOLSURF program.

Relative Binding Affinity Assay—Relative binding affinities were determined by competitive radiometric binding assays with 2 nM [^{3}H]E_2 as tracer, as a modification of methods previously described.[14] The source of ER was purified full-length human ERα and ERβ purchased from Pan Vera/Invitrogen (Carlsbad, CA). Incubations were done at 0 °C for 18–24 h, and hydroxyapatite was used to absorb the purified receptor–ligand complexes (human ERs).[14b] The binding affinities are expressed as relative binding affinity (RBA) values, where the RBA of estradiol is 100%; under these conditions, the K_d of estradiol for ERα is ~0.2 nM, and for ERβ it is 0.5 nM. The determination of these RBA values is reproducible in separate experiments with a CV of 0.3, and the values shown represent the average ± range or SD of two or more separate determinations.

Tr-FRET assays

Protein Preparation—The ligand binding domains (LBD) of the human ERα (amino acids 304–554), the human ERβ (amino acids 256–503), and the nuclear receptor domain (NRD) of human SRC3 encompassing three NR boxes (amino acids 627–829) were expressed in *E. coli*, using methods reported previously.[19, 30] The ER proteins were prepared as His_6 fusion proteins, with a single reactive cysteine at C417 (ERα) or C369 (ERβ).[30] While bound to the Ni-NTA-agarose resin (Qiagen, inc, Santa Clarita, CA), the ERs were labeled with MAL-dPEG4-biotin (Quanta BioDesign, Powell, OH). The SRC3-NRD construct has 4 cysteines and was labeled non-specifically with 5-iodoacetamido fluorescein, also while on the resin (Molecular Probes/Invitrogen, Eugene. OR).[19] It has been previously determined that an average of 1.8–2 cysteines were labeled.[31]

SRC titration—SRC3 was titrated into a fixed amount of ER-LBD-biotin mixed with SaTb (streptavidin-terbium, Invitrogen, Grand Island, NY), on 96-well black microplates (Molecular Devices, Sunnyvale, CA), following previously determined methods.[16, 20] The time-resolved Fluorescence Resonance Energy Transfer (tr-FRET) was measured with a Victor X5 plate reader (Perkin Elmer, Shelton, CT) with an excitation filter at 340/10 nm and emission filters for terbium and fluorescein at 495/20 and 520/25 nm, respectively, with a 100 μs delay. Diffusion-enhanced FRET was determined by a parallel incubation without biotinylated ER-LBD and subtracted as a background. The final concentrations of reagents were: 1 nM ER-LBD-biotin, 0.25 nM streptavidin-terbium, 1 μM ligand, SRC3 coactivator titrated from 3.2×10^{-7} to 3.2×10^{-12} M. The data, representing two to three replicate

experiments, each with duplicate points, was analyzed using GraphPad Prism 4 and is expressed as the EC_{50} in nM.

Ligand titration—Ligands were titrated into a constant amount of ER-LBD-biotin, SaTb, SRC3. The final concentrations were 1 nM ER-LBD, 0.25 nM SaTb, 100 nM SRC3-fluorescein and increasing ligand concentrations from 1×10^{-6} to 1×10^{-12} M. Diffusion-enhanced FRET was determined by a parallel incubation without biotinylated ER-LBD and subtracted as a background. The tr-FRET was measured with a Victor X5 plate reader, as outlined above. The data, representing two to three replicate experiments, each with duplicate points, was analyzed using GraphPad Prism 4, and is expressed as the EC_{50} in nM.

Cell Viability assays—U87, LoVo, HCT, MDA-MB-231, MCF7, SkBr3 were maintained at 37 °C in a humidified atmosphere containing 5% CO_2 accordingly to the supplier. Cells (10^3) were plated in 96-well culture plates. The day after seeding, vehicle or compounds were added at different concentrations to the medium at a concentration ranging from 1000 to 0.1 μM. Cell viability was measured after 96 h according to the supplier (Promega, G7571) with a Tecan F200 instrument. IC_{50} values were calculated from logistical dose response curves. Averages and standard errors were obtained from three different experiments.

Supplementary Material

Refer to Web version on PubMed Central for supplementary material.

Acknowledgments

Intramural funding support from the University of Pisa (to F.M.) and support from the National Institutes of Health (Grant PHS 5R01 DK015556 to J.A.K.) are gratefully acknowledged. The Q-Tof Ultima mass spectrometer was purchased in part with a grant from the National Science Foundation, Division of Biological Infrastructure (DBI-0100085).

Abbreviations

ER	estrogen receptor
LBD	ligand binding domain
E_2	estradiol
RBA	relative binding affinity
ERE	estrogen response element
SRC3	steroid receptor coactivator 3
SD	standard deviation
tr-FRET	time resolved-fluorescence resonance energy transfer
NRID	nuclear receptor interaction domain

SaTb	streptavidin-terbium
RMSD	root-mean-square deviation
MD	molecular dynamic
MM-PBSA	molecular mechanics-poisson bolzmann surface area
SAR	structure-activity relationships
ppm	parts per million
NMR	nuclear magnetic resonance
TLC	thin layer chromatography
rt	room temperature
EI	electron impact
HRMS	high-resolution mass spectrometry
s	singlet
d	doublet
dd	double doublet
ddd	double double doublet
t	triplet
m	multiplet
bs	broad signal

References

1. Dahlman-Wright K, Cavailles V, Fuqua SA, Jordan VC, Katzenellenbogen JA, Korach KS, Maggi A, Muramatsu M, Parker MG, Gustafsson J-Å. International Union of Pharmacology. LXIV. Estrogen Receptors. Pharmacol Rev. 2006; 58:773–781. [PubMed: 17132854]
2. Chang EC, Frasor J, Komm B, Katzenellenbogen BS. Endocrinology. 2006; 147:4831–4842. [PubMed: 16809442]
3. McPherson SJ, Hussain S, Balanathan P, Hedwards SL, Niranjan B, Grant M, Chandrasir UP, Toivanen R, Wang Y, Taylor RA, Risbridger GP. Proc Natl Acad Sci USA. 2010; 107:3123–3128. [PubMed: 20133657]
4. Hartman J, Edvardsson K, Lindberg K, Zhao C, Williams C, Strom A, Gustafsson J-Å. Cancer Res. 2009; 69:6100–6106. [PubMed: 19602591]
5. Yu CP, Ho JY, Huang YT, Cha TL, Sun GH, Yu DS, Chang FW, Chen SP, Hsu RJ. PLoS One. 2013; 8:e56667. [PubMed: 23460808]
6. Pinton G, Thomas W, Bellini P, Manente AG, Favoni RE, Harvey BJ, Mutti L, Moro L. PLoS One. 2010; 5:e14110. [PubMed: 21124760]
7. Sareddy GR, Nair BC, Gonugunta VK, Zhang QG, Brenner A, Brann DW, Tekmal RR, Vadlamudi RK. Mol Cancer Ther. 2012; 11:1174–1182. [PubMed: 22442308]

8. Kuiper GGJM, Enmark E, Pelto-Huikko M, Nilsson S, Gustafsson J-Å. Proc Natl Acad Sci USA. 1996; 93:5925–5930. [PubMed: 8650195]
9. a) Minutolo F, Macchia M, Katzenellenbogen BS, Katzenellenbogen JA. Med Res Rev. 2011; 31:364–442. [PubMed: 19967775] b) Paterni I, Granchi C, Katzenellenbogen JA, Minutolo F. Steroids. 2014; 90:13–29. [PubMed: 24971815]
10. Paterni I, Bertini S, Granchi C, Tuccinardi T, Macchia M, Martinelli A, Caligiuri I, Toffoli G, Rizzolio F, Carlson KE, Katzenellenbogen BS, Katzenellenbogen JA, Minutolo F. J Med Chem. 2015; 58:1184–1194. [PubMed: 25559213]
11. a) Minutolo F, Bellini R, Bertini S, Carboni I, Lapucci A, Pistolesi L, Prota G, Rapposelli S, Solati F, Tuccinardi T, Martinelli A, Stossi F, Carlson KE, Katzenellenbogen BS, Katzenellenbogen JA, Macchia M. J Med Chem. 2008; 51:1344–1351. [PubMed: 18269232] b) Minutolo F, Bertini S, Granchi C, Marchitiello T, Prota G, Rapposelli S, Tuccinardi T, Martinelli A, Gunther JR, Carlson KE, Katzenellenbogen JA, Macchia M. J Med Chem. 2009; 52:858–867. [PubMed: 19128016] c) Bertini S, DeCupertinis A, Granchi C, Bargagli B, Tuccinardi T, Martinelli A, Macchia M, Gunther JR, Carlson KE, Katzenellenbogen JA, Minutolo F. Eur J Med Chem. 2011; 46:2453–2462. [PubMed: 21481497]
12. Granchi C, Qian Y, Lee HY, Paterni I, Pasero C, Iegre J, Carlson KE, Tuccinardi T, Chen X, Katzenellenbogen JA, Hergenrother PJ, Minutolo F. ChemMedChem. 2015; 10:1892–1900. [PubMed: 26332543]
13. Ngwerume S, Camp JE. J Org Chem. 2010; 75:6271–6274. [PubMed: 20718448]
14. a) Katzenellenbogen JA, Johnson HJ Jr, Myers HN. Biochemistry. 1973; 12:4085–4092. [PubMed: 4745660] b) Carlson KE, Choi I, Gee A, Katzenellenbogen BS, Katzenellenbogen JA. Biochemistry. 1997; 36:14897–14905. [PubMed: 9398213]
15. a) Sun J, Meyers MJ, Fink BE, Rajendran R, Katzenellenbogen JA, Katzenellenbogen BS. Endocrinology. 1999; 140:800–804. [PubMed: 9927308] b) Meyers MJ, Sun J, Carlson KE, Kazenellenbogen BS, Katzenellenbogen JA. J Med Chem. 1999; 42:2456–2468. [PubMed: 10395487]
16. Gunther JR, Du Y, Rhoden E, Lewis I, Revennaugh B, Moore TW, Kim SH, Dingledine R, Fu H, Katzenellenbogen JA. J Biomol Screening. 2009; 14:181–193.
17. Hilal T, Puetter V, Otto C, Parczyk K, Bader B. J Biomol Screening. 2010; 15:268–278.
18. Lascombe I, Beffa D, Ruegg U, Tarradellas J, Wahli W. Environ Health Perspect. 2000; 108:621–629. [PubMed: 10903615]
19. Tamrazi A, Carlson KE, Rodriguez AL, Katzenellenbogen JA. Mol Endocrinol. 2005; 19:1516–1528. [PubMed: 15661830]
20. Jeyakumar M, Carlson KE, Gunther JR, Katzenellenbogen JA. J Biol Chem. 2011; 286:12971–12982. [PubMed: 21321128]
21. Tamrazi A, Carlson KE, Katzenellenbogen JA. Mol Endocrinol. 2003; 17:2593–2602. [PubMed: 12947047]
22. Kollman PA, Massova I, Reyes C, Kuhn B, Huo S, Chong L, Lee M, Lee T, Duan Y, Wang W, Donini O, Cieplak P, Srinivasan J, Case DA, Cheatham TE 3rd. Acc Chem Res. 2000; 33:889–897. [PubMed: 11123888]
23. Tuccinardi T, Manetti F, Schenone S, Martinelli A, Botta M. J Chem Inf Model. 2007; 47:644–655. [PubMed: 17295463]
24. Norman BH, Dodge JA, Richardson TI, Borromeo PS, Lugar CW, Jones SA, Chen K, Wang Y, Durst GL, Barr RJ, Montrose-Rafizadeh C, Osborne HE, Amos RM, Guo S, Boodhoo A, Krishnan V. J Med Chem. 2006; 49:6155–6157. [PubMed: 17034120]
25. Berman HM, Westbrook J, Feng Z, Gilliland G, Bhat TN, Weissig H, Shindyalov IN, Bourne PE. Nucleic Acids Res. 2000; 28:235–242. [PubMed: 10592235]
26. Morris GM, Huey R, Lindstrom W, Sanner MF, Belew RK, Goodsell DS, Olson AJ. J Comp Chem. 2009; 30:2785–2791. [PubMed: 19399780]
27. Sanner MF. J Mol Graph Model. 1999; 17:57–61. [PubMed: 10660911]
28. Case, DA.; Berryman, JT.; Betz, RM.; Cerutti, DS.; Cheatham, TE., III; Darden, TA.; Duke, RE.; Giese, TJ.; Gohlke, H.; Goetz, AW.; Homeyer, N.; Izadi, S.; Janowski, P.; Kaus, J.; Kovalenko, A.; Lee, TS.; LeGrand, S.; Li, P.; Luchko, T.; Luo, R.; Madej, B.; Merz, KM.; Monard, G.; Needham,

P.; Nguyen, H.; Nguyen, HT.; Omelyan, I.; Onufriev, A.; Roe, DR.; Roitberg, A.; Salomon-Ferrer, R.; Simmerling, CL.; Smith, W.; Swails, J.; Walker, RC.; Wang, J.; Wolf, RM.; Wu, X.; York, DM.; Kollman, PA. AMBER. University of California; San Francisco: 2015.

29. Essmann U, Perera L, Berkowitz ML, Darden TA, Lee H, Pedersen LG. J Chem Phys. 1995; 103:8577–8594.
30. Tamrazi A, Carlson KE, Daniels JR, Hurth KM, Katzenellenbogen JA. Mol Endocrinol. 2002; 16:2706–2719. [PubMed: 12456792]
31. Kim SH, Tamrazi A, Carlson KE, Katzenellenbogen JA. Mol Cell Proteomics. 2005; 4:267–277. [PubMed: 15613364]

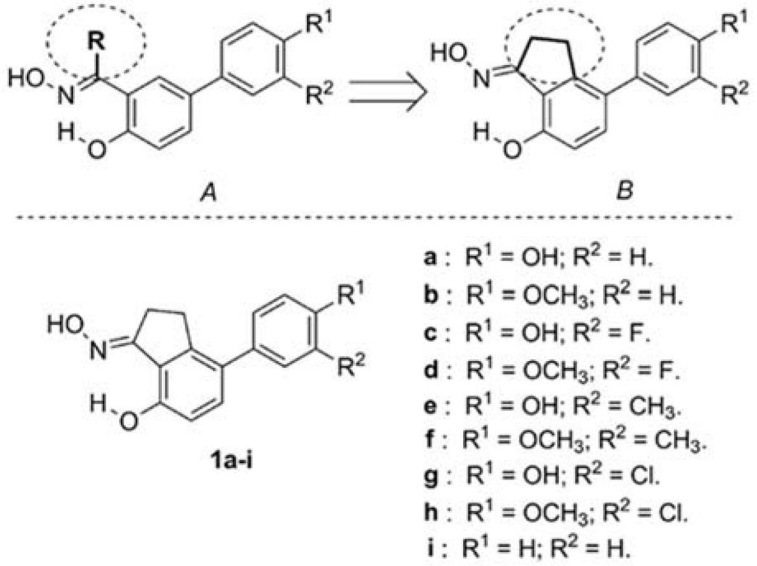

Figure 1.

General structures of salicylketoximes *A* and *B* (upper part); structures of the newly synthesized salicylketoximes **1a–i** (lower part).

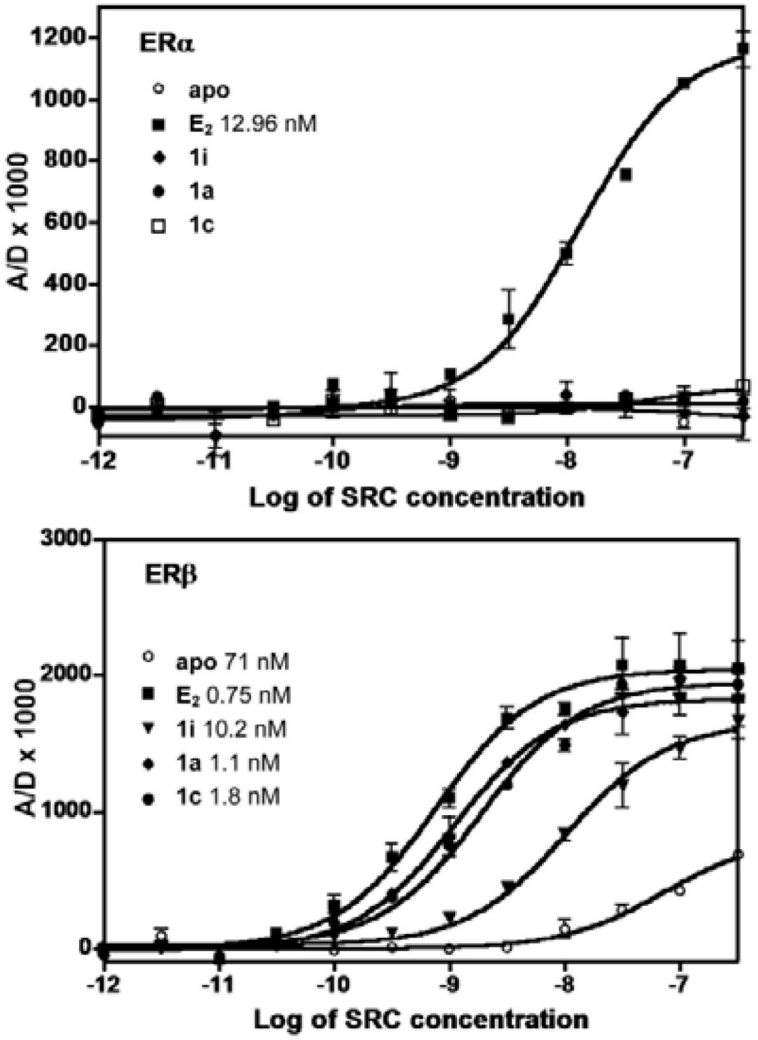

Figure 2.

Experiment of SRC-fluorescein titration into a constant amount of ER and ligand to measure the affinity of SRC binding to an ER-ligand complex. The upper graph is with ERα and the lower one is with ERβ. Values are the mean ± SD of duplicate to triplicate determinations, each with duplicate points.

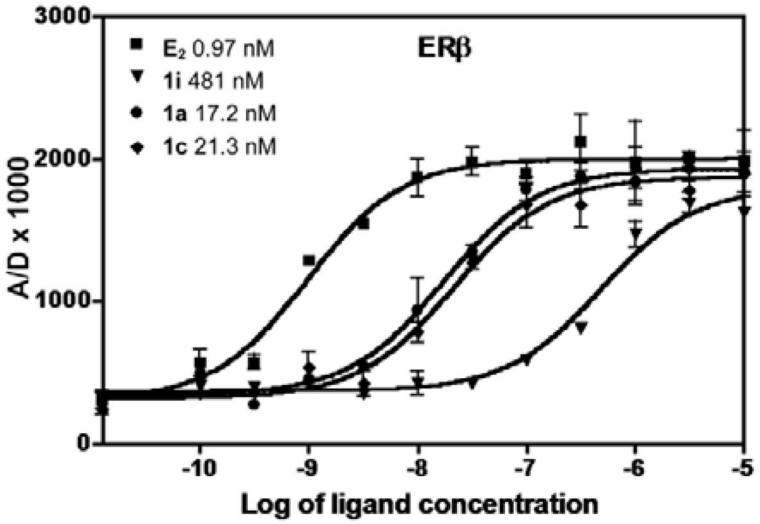

Figure 3.

Experiment of ligand titration into a constant amount of ERβ and SRC3 to measure ligand potency in coactivator recruitment. Values are the mean ± SD of duplicate to triplicate determinations, each with duplicate points.

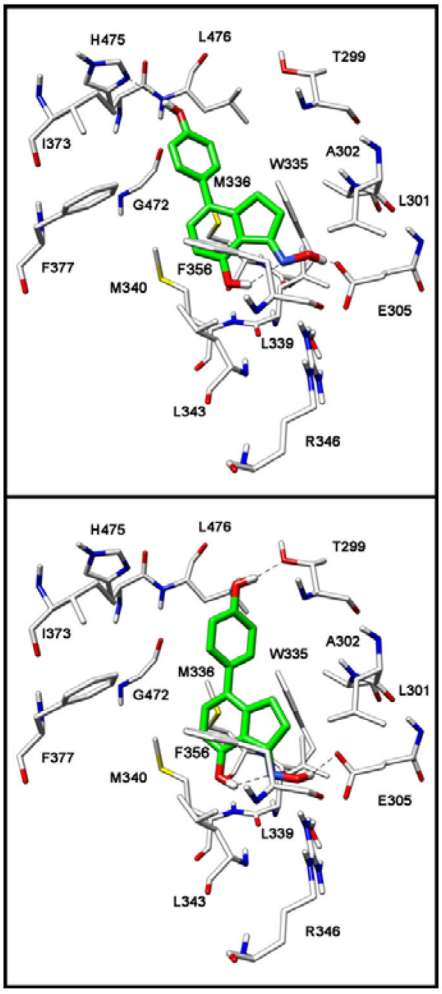

Figure 4.
Docking of compound **1a** into ERβ. Binding mode A (upper part) and binding mode B (lower part).

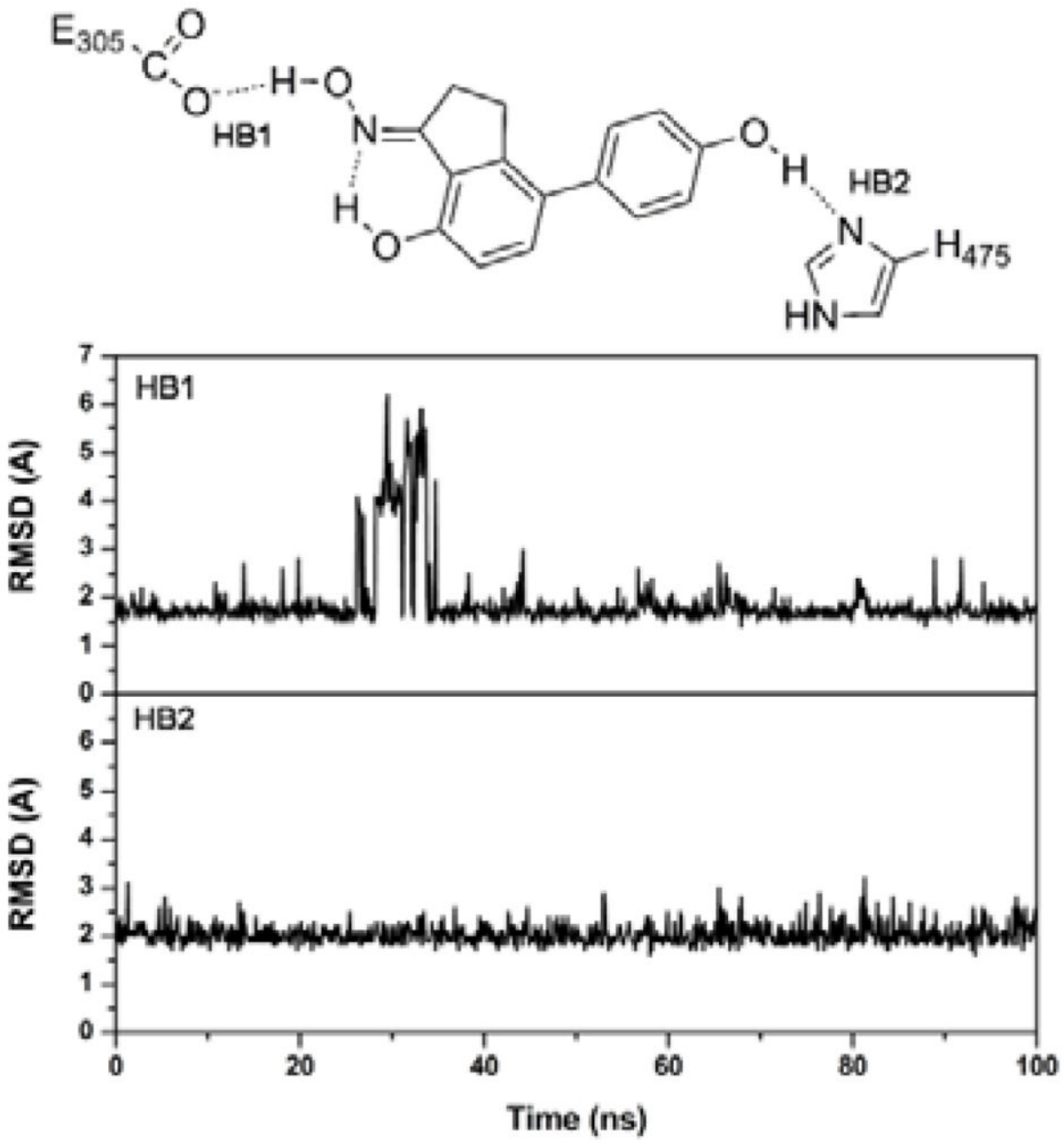

Figure 5.

Analysis of the ERβ-**1a** MD simulation (binding mode A). The plots show the distance analysis for the two H-bonds (HB1 and HB2, respectively).

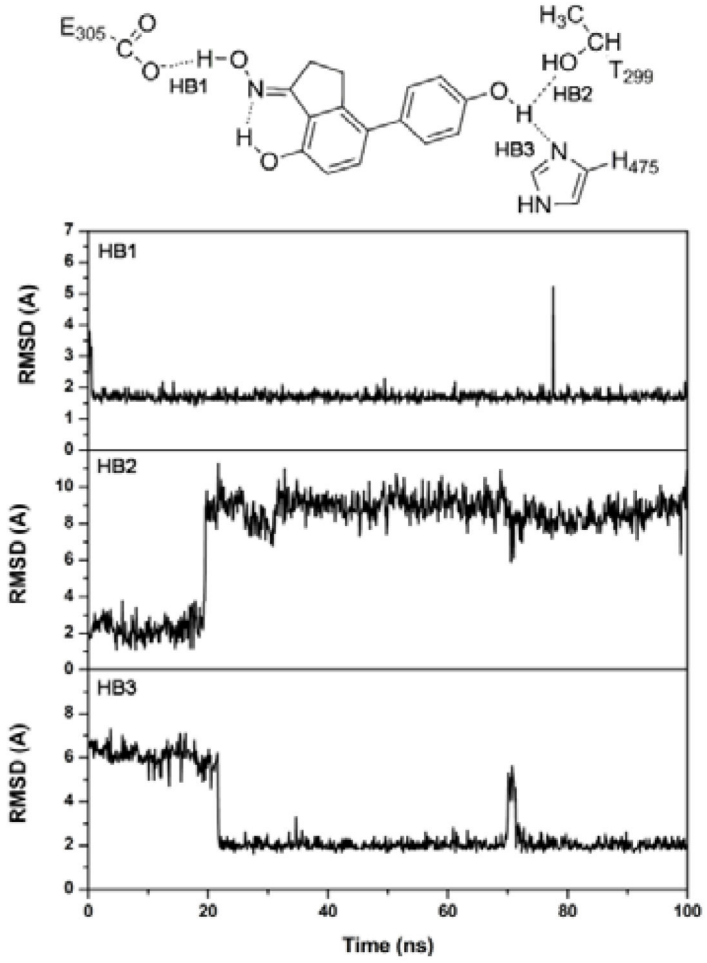

Figure 6.

Analysis of the ERβ-**1a** MD simulation (binding mode B). The plots show the distance analysis for the three H-bonds (HB1, HB2 and HB3, respectively).

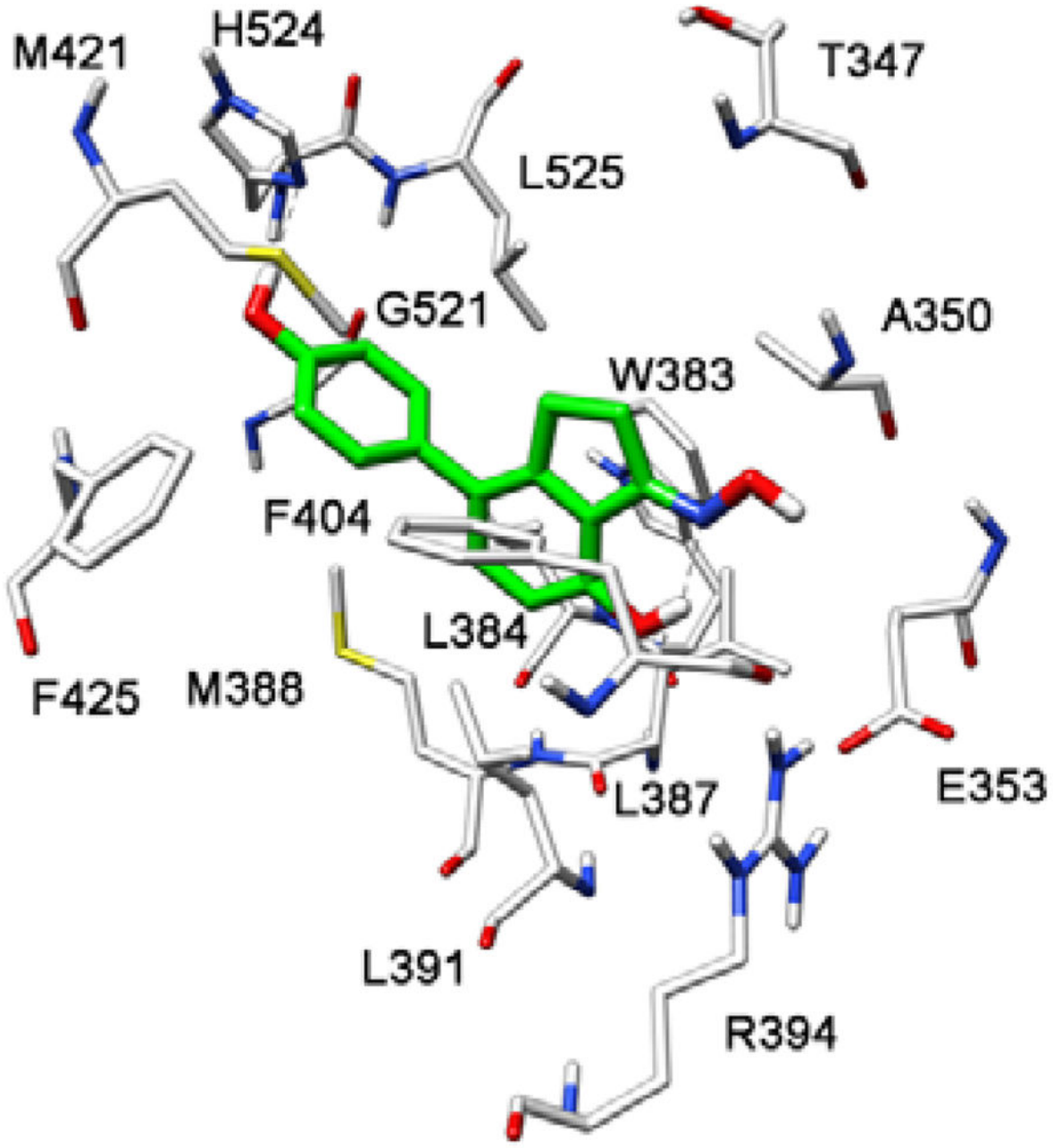

Figure 7.
Minimized average structure of compound **1a** docked into ERα.

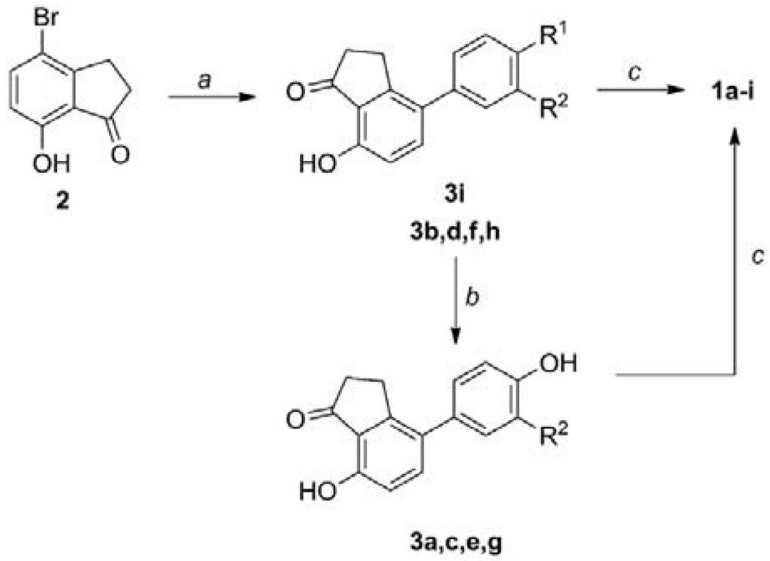

Scheme 1.

Synthesis of salicylketoximes **1a–i**. *Reagents and conditions*: (a) $ArB(OH)_2$, $Pd(OAc)_2$, PPh_3, aqueous 2 M Na_2CO_3, 1:1 toluene/EtOH, 100 °C, 24 h; (b) BBr_3, CH_2Cl_2, −78 to 0 °C, 1 h; (c) $NH_2OH{\cdot}HCl$, EtOH-H_2O, 50 °C, 24 h.

Table 1

Relative Binding Affinities[a] of Cyclic Ketoximes **1a–i** for the Estrogen Receptors α and β (RBA, %)

Ligand	ERα	ERβ	β/α ratio
Estradiol	(100)	(100)	1
1a	0.261 ± 0.060	4.28 ± 0.62	16
1b	0.003 ± 0.001	0.009 ± 0.002	3.0
1c	0.143 ± 0.040	4.71 ± 0.46	33
1d	0.005 ± 0.001	0.004 ± 0.001	0.8
1e	0.202 ± 0.020	1.26 ± 0.26	6.3
1f	0.003 ± 0.001	0.003 ± 0.000	1.0
1g	0.024 ± 0.004	0.192 ± 0.050	8.0
1h	0.004 ± 0.001	0.002 ± 0.000	0.50
1i	0.002 ± 0.000	0.177 ± 0.040	89

[a]Determined by a competitive radiometric binding assay with [^{3}H]estradiol. Preparations of purified, full-length human ERα and ERβ (PanVera) were used; see Experimental Section. Values are reported as the mean ± the range or SD of two or more independent experiments. The K_d of estradiol for ERα is 0.2 nM and for ERβ is 0.5 nM. K_i values for the new compounds can be readily calculated by using the formula $K_i = (K_d[\text{estradiol}]/\text{RBA}) \times 100$.

Table 2

EC_{50} values for SRC binding to ERβ-ligand complexes from SRC titration experiments. Values are reported as the mean ± SD of two or more independent experiments.

EC_{50} (nM)				
Apo	**E_2**	**1a**	**1c**	**1i**
75 ± 5	0.64 ± 0.16	0.99 ± 0.16	1.69 ± 0.16	10.5 ± 0.4

Table 3

ERβ-RBA values, EC_{50} values for SRC binding to ERβ-ligand complexes by SRC titration, and EC_{50} values for ligand recruitment of SRC to ERβ from ligand titration experiments. For comparison, ERβ-RBA values are converted to K_i values. Values are reported as the mean ± SD of two or more independent experiments.

Ligand	ERβ-RBA	SRC binding affinity (SRC titration) EC_{50} (nM)	Ligand coactivator recruitment potency (Ligand titration) EC_{50} (nM)	ERβ binding affinity K_i (nM)[a]	Efficacy %
E_2	100	0.64 ± 0.16	1.10 ± 0.13	0.50	100
1a	4.28 ± 0.62	0.99 ± 0.16	14.2 ± 3.0	11.7	93
1c	4.71 ± 0.46	1.69 ± 0.16	19.5 ± 2.6	10.6	88
1i	0.177 ± 0.040	10.5 ± 0.4	393 ± 124	282	72

[a] Calculated from RBA values by applying the formula: $K_i = (K_d (E_2) \times 100)/RBA$; K_d of estradiol on ERβ = 0.50 nM.

Table 4

Effects on cell growth (IC_{50}, μM) of human glioma (U87), colon (LoVo, HCT), and breast (MDA-MB-231, MCF7, SkBr3) cancer cells by compounds 1**a**, 1**c** and **Liquiritigenin**[a]

Ligand	U87	LoVo	HCT	MDA231	MCF7	SkBr3
Liquiritigenin	115.0 ± 11.7	101.3 ± 10.2	75.3 ± 7.1	143.7 ± 14.5	> 250	154.6 ± 7.4
1a	150.7 ± 1.2	19.8 ± 2.1	61.5 ± 8.8	42.3 ± 1.1	70.1 ± 12.4	139.9 ± 11.2
1c	32.3 ± 1.1	14.5 ± 3.1	10.8 ± 1.2	8.1 ± 1.3	23.2 ± 1.4	130.4 ± 9.7

[a] IC_{50}: inhibitory concentrations causing a 50% reduction in cell growth, in μM. Mean values ± SD calculated from at least two triplicate cytotoxicity experiments (see Experimental section).